Preprint typeset using LaTeX style emulateapj v. 12/16/11

PLANETARY CANDIDATES FROM *K2* CAMPAIGN 16

Liang Yu[1], Ian J. M. Crossfield[1], Joshua E. Schlieder[2], Molly R. Kosiarek[3,†], Adina D. Feinstein[4], John H. Livingston[5], Andrew W. Howard[6], Björn Benneke[7], Erik Petigura[6,⋆], Charles A. Beichman[8], David A. Berardo[1], Makennah Bristow[9], Jessie L. Christiansen[8], David R. Ciardi[8], Justin Crepp[9], Courtney D. Dressing[10], Benjamin J. Fulton[7,‡], Erica J. Gonzales[3], Kevin K. Hardegree-Ullman[11], Thomas Henning[12], Howard Isaacson[10], Heather A. Knutson[7], Sébastien Lépine[13], Arturo O. Martinez[14], Farisa Y. Morales[15,16], Rahul I. Patel[8], Evan Sinukoff[6,17], Michael W. Werner[15]

ABSTRACT

We present a catalog of interesting targets recently identified using data from Campaign 16 of the *K2* mission. Our catalog includes 32 high-quality planet candidates (showing no signs of being non-planetary in nature), 54 more ambiguous events that may be either planets or false positives, 169 eclipsing binaries, and 217 other regularly periodic variable sources. We have released light curves for all targets in C16, and have also released system parameters and transit vetting plots for all interesting candidates identified in this paper. Of particular interest is a candidate planet orbiting the bright F dwarf HD 73344 ($V = 6.9$, $K = 5.6$) with an orbital period of 15 days. If confirmed, this object would correspond to a $\sim 2.6\ R_\oplus$ planet and would likely be a favorable target for radial velocity characterization. Campaign 16 is one of just two *K2* campaigns observed so far in "forward-facing" mode, which enables immediate follow-up observations from the ground. This paper is intended as a rapid release of planet candidates, eclipsing binaries and other interesting periodic variables to maximize the scientific yield of this campaign, and as a test run for the upcoming *TESS* mission, whose frequent data releases call for similarly rapid candidate identification and efficient follow-up.

Subject headings: methods: data analysis, planets and satellites: detection, techniques: photometric

1. INTRODUCTION

By any measure, NASA's *K2* mission (Howell et al. 2014) has been a success. Out of the ashes of an ailing spacecraft has risen a tremendously productive scientific mission. Sometime this year *K2* will likely run out of the propellant needed to maintain its stable pointing and deliver precise time-series photometry. 2018 is perhaps an appropriate year for this event, since it marks the 40 year anniversary of the first American summit of K2 — the "Savage Mountain" — which itself occurred 40 years after an American team first demonstrated the feasibility of climbing that peak. Hundreds of planets and other astrophysical phenomena have been studied with *K2*, far fewer than the thousands discovered by the original *Kepler* mission (Thompson et al. 2017) — just as thousands of climbers have summitted Mount Everest even though only hundreds have ever reached the top of K2. Nonetheless, even after the mission ends, an enduring kinship will remain between those who have been fortunate enough to use *K2* in their research efforts.

In that same communal spirit, we provide a rapid, public release of light curves, planet candidates, and other interesting periodic variables from *K2*'s Campaign 16 (C16) in this paper. Unlike most fields observed by *K2*, C16 was observed in "forward-facing" mode, meaning that the field was observable throughout the night as soon as the campaign ended. We have conducted this quick-look analysis of uncalibrated C16 cadence data and are releasing these data products in order to maximize the scientific yield of what could be *K2*'s final campaign. We hope that this will also provide a test for the imminent *TESS* mission, whose frequent data releases will also benefit from rapid candidate identification and follow-up.

In the following sections we describe our procedures and results. In Sec. 2, we describe how we compute time-series photometry and search for transit-like sig-

[1] Department of Physics, and Kavli Institute for Astrophysics and Space Research, Massachusetts Institute of Technology, Cambridge, MA 02139, USA
[2] NASA Goddard Space Flight Center, 8800 Greenbelt Road, Greenbelt, MD 20771, USA
[3] Department of Astronomy and Astrophysics, University of California, Santa Cruz, CA 95064, USA
[4] Department of Physics and Astronomy, Tufts University, Medford, MA 02155, USA
[5] Department of Astronomy, Graduate School of Science, The University of Tokyo, Hongo 7-3-1, Bunkyo-ku, Tokyo, 113-0033, Japan
[6] Cahill Center for Astrophysics, California Institute of Technology, Pasadena, CA 91125, USA
[7] Division of Geological and Planetary Sciences, California Institute of Technology, Pasadena, CA 91125, USA
[8] Caltech/IPAC-NASA Exoplanet Science Institute, 770 S. Wilson Ave, Pasadena, CA 91106, USA
[9] Department of Physics, University of North Carolina at Asheville, Asheville, NC 28804, USA
[9] Department of Physics, University of Notre Dame, Notre Dame, IN 46556, USA
[10] Department of Astronomy, University of California, Berkeley, CA 94720, USA
[11] The University of Toledo, 2801 West Bancroft Street, Mailstop 111, Toledo, OH 43606, USA
[12] Max Planck Institute for Astronomy, Königstuhl 17, D-69117 Heidelberg, Germany
[13] Department of Physics & Astronomy, Georgia State University, 25 Park Place NE 605, Atlanta, GA 30303, USA
[14] Department of Astronomy, San Diego State University, 5500 Campanile Drive, San Diego, CA 92182, USA
[15] Jet Propulsion Laboratory, California Institute of Technology, 4800 Oak Grove Drive, Pasadena, CA 91109, USA
[16] Department of Physical Sciences, Moorpark College,7075 Campus Road, Moorpark, CA 93021, USA
[17] Institute for Astronomy, University of Hawai'i, Honolulu, HI 96822, USA
[†] NSF Graduate Research Fellow
[⋆] NASA Hubble Fellow
[‡] Texaco Fellow

nals. Sec. 3 then discusses our approach for discriminating between various astrophysical signals and measurement noise. Finally, in Sec. 4 we conclude by discussing several particularly interesting systems and reviewing the overall C16 candidate sample.

2. *K2* TARGETS AND PHOTOMETRY

2.1. *Target Selection and C16 Data Characteristics*

K2 target selection is entirely community driven, with all targets selected from Guest Observer (GO) proposals. Our team has proposed large samples of F, G, K, and M dwarfs for every *K2* Campaign up to Campaign 17, but in the analysis that follows we use data from all *K2* GO proposals to maximize the science yield from this campaign.

During C16, *K2* observed 20647 stars in a field centered at RA = 08:54:50, Dec = +18:31:31, for a period of 80 days between 2017 Dec 07 and 2018 Feb 25. This is only the second campaign in which the spacecraft was pointed along the forward-facing direction of its velocity vector (the other, C9, was dedicated mostly to microlensing and was in a dense field unsuited for standard transit searches). Forward-facing observations enable simultaneous observations from the ground and with *K2*, and also allow the field to be accessed from ground-based observatories as soon as compelling targets can be identified. C16 also overlaps with C5 except for a 40 px-wide strip that is not on silicon in C16. C16 therefore includes dozens of confirmed and candidate planets from C5, some of which we rediscover in our analysis.

2.2. *Time-Series Photometry*

Raw cadence pixel data for C16 became available on the Mikulski Archive for Space Telescopes (MAST)[22] on 2018 Feb 28. We first convert the raw cadence data into target pixel files with `kadenza`[23] (Barentsen 2018), following the approach described in Christiansen et al. (2018).

From then on we process the data using a photometric pipeline that has been described in detail in past works by members of our team (e.g. Crossfield et al. 2015; Petigura et al. 2015, 2018). In brief, we follow an approach similar to that originally outlined by Vanderburg & Johnson (2014). We compute the raw photometry by summing the flux within a soft-edged, stationary, circular aperture centered on each target star. During *K2* operations, solar radiation pressure causes the telescope to roll around its boresight. Consequently, stars trace out small arcs of up to several pixels every $\sim$ 6 hr. Interpixel sensitivity variations and aperture losses can then lead to significant changes in the brightness of stars that dominate *K2* photometry.

To correct for these motion-dependent systematics, we solve for the roll angle between each frame and an arbitrary reference frame using roughly 100 stars of Kepler magnitude $Kp \sim 12$ mag on an arbitrary output channel (we typically use channel 4). Then we use the publicly available `k2phot` photometry code[24] to model the time- and roll-dependent brightness variations using a Gaussian process with a squared-exponential kernel. The models can be individually applied to the raw photometry to produce photometry corrected for motion-dependent systematics or fully detrended photometry. Fig. 1 shows an example of raw *K2* photometry for a relatively well-behaved star, along with the same light curve after correction for systematics and subsequent detrending. Some light curves with relatively deep transits, as in this example, show small increases in flux immediately before and after the transits. These are artifacts from the detrending process. The transits are effectively outliers on short timescales that may bias the Gaussian process model, leading to overfitting.

We repeat this photometry process for apertures with radii ranging from 1 to 7 pixels, and also fit a custom, automatically-generated aperture that selects pixels based on how much flux they receive relative to the background. This aperture has an irregular shape and captures most of the flux from each target. For each target we adopt the aperture that minimizes the residual noise on 3 hr timescales. Specifically, we use the median absolute deviation (MAD) of the 3 hr Single Event Statistic (SES) as our noise metric. We define the SES as the depth of a box-shaped dimming relative to the local photometric level. This method of aperture selection favors smaller apertures, which incur less background noise, for fainter stars and larger apertures for brighter targets. For strongly saturated stars the custom aperture is typically chosen, since in these cases circular apertures miss substantial flux.

2.3. *Transit Search*

We search our calibrated photometry for transit signals using the publicly available `TERRA` algorithm[25] (Petigura et al. 2013a,b). `TERRA` flags targets with putative transits as threshold-crossing events (TCEs), which we later examine visually (see Sec. 3). Once a TCE is detected, `TERRA` automatically runs again to search for additional signals in the same system (see Sinukoff et al. 2016) until no more TCEs are found or until the number of candidates exceeds 5.

Many spurious detections at lower S/N are caused by residual outliers in the photometry. In order to reduce the number of spurious detections, we require that TCEs have orbital periods longer than 0.5 d, and that they also show at least three transits. This last criterion rules out any planets with periods longer than half the campaign baseline, or $\sim$ 40 days. Thus many longer-period planets likely remain to be found in this data set. Furthermore, we adopt a threshold of S/N$\geq$ 12 to yield a good balance between sensitivity to shallow transits and the number of spurious detections. In previous catalog papers produced using the fully processed target pixel files released later by the *K2* project office, we typically vetted candidates down to a lower S/N threshold of 10. We find that spurious detections are more frequent in light curves derived from uncalibrated cadence data than when using fully calibrated pixel files.

In total, `TERRA` produced a list of 1097 TCEs in C16 with nominal S/N$\geq$12. The distribution of their orbital periods is shown in Fig. 2.

[22] https://archive.stsci.edu/k2/
[23] https://github.com/KeplerGO/kadenza
[24] https://github.com/petigura/k2phot
[25] https://github.com/petigura/terra

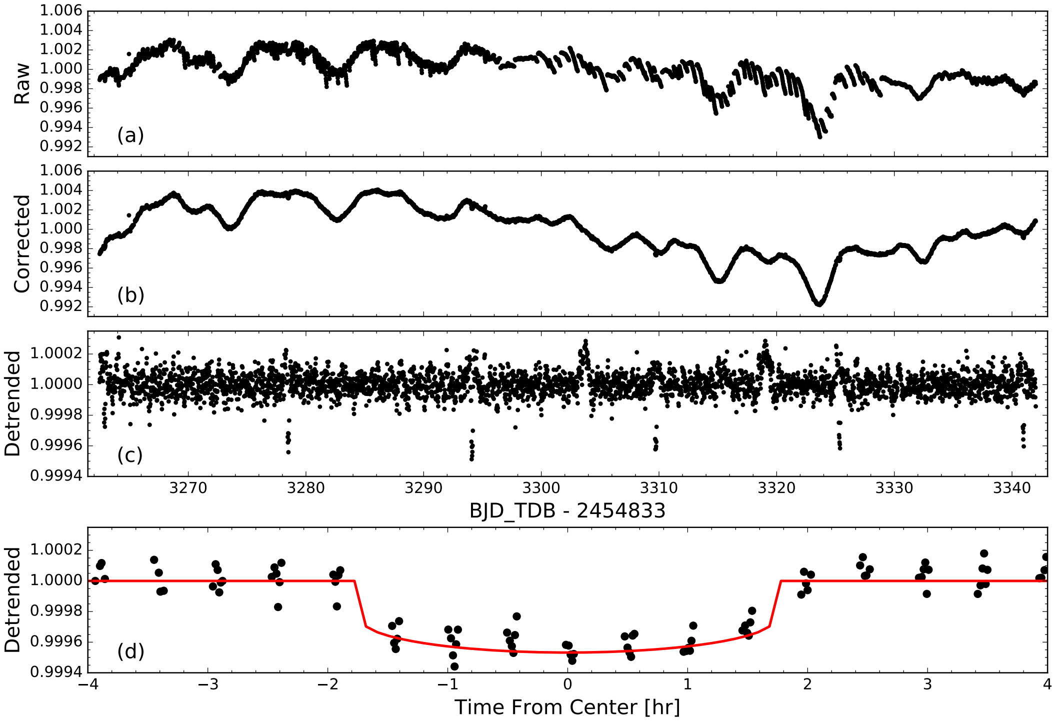

FIG. 1.— *K2* photometry of HD 73344 (V = 6.9) and its planet candidate, EPIC 212178066.01. From top to bottom: raw aperture photometry; after removal of telescope systematics, revealing a likely 8.5±0.5 d rotation period; after detrending, clearly revealing candidate transits; and after phase-folding and overplotting a model transit profile (red). The bumps in panel (c) do not occur on the same period as the candidate transit and may be artifacts of the detrending process.

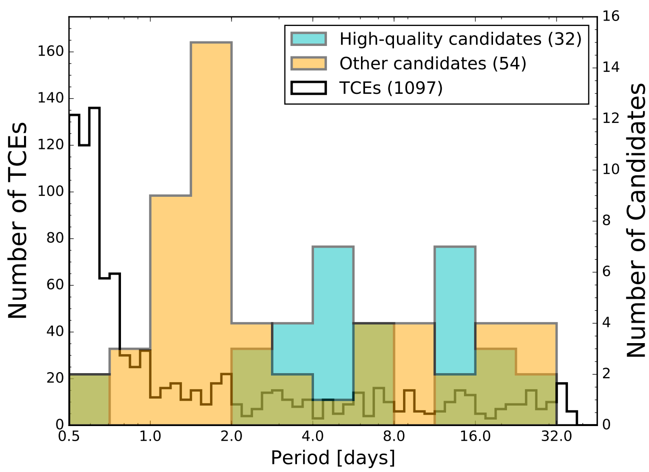

FIG. 2.— Orbital periods of transit-like signals identified in our analysis. The unfilled, narrow-binned histogram (axis at left) shows the Threshold-Crossing Events (TCEs) identified by `TERRA` in our initial transit search (see Sec. 2.3). The coarser histograms (axis at right) indicate the distributions of 32 high-quality candidates (blue-green) and 54 remaining, plausibly planetary candidates (orange).

3. TRIAGE AND VETTING

The majority of TCEs identified by `TERRA` are not caused by genuine transiting planets, but instead by residual instrumental artifacts, eclipsing binary stars, or other periodic stellar variability (e.g. pulsations and spot modulations). We manually vet our entire list of 1097 TCEs to differentiate between these various signals. This process results in a list of robust planet candidates for further follow-up and validation, as well as a list of eclipsing binaries and other periodically variable sources.

We promote TCEs showing no obvious warning signs to the status of "planet candidate" in the spirit of "Kepler Objects of Interest" (KOIs), i.e. events that are almost certainly astrophysical in nature and not obviously false positive scenarios such as eclipsing binaries or variable stars. Details of the vetting process are described in Crossfield et al. (2016) and Petigura et al. (2018). `TERRA` produces a set of diagnostics for every TCE, which we use to classify the event as a candidate planet, eclipsing binary, periodic variable, or noise. The diagnostics include a summary of basic fit parameters and a suite of diagnostic plots to visualize the nature of the TCE. These plots include the `TERRA` periodogram, a normalized phase-folded light curve with the best-fit Mandel & Agol (2002) model, the light curve phased to 180° to look for eclipses or misidentified periods, the most probable secondary eclipse identified at any phase, and an autocorrelation function. In the era of *TESS*, cross-matching to ground-based surveys will be another excellent way to discover false positives (e.g. Oelkers et al. 2018).

Table 2 lists the 32 highest-quality planet candidates whose light curves (shown in Fig. 3) show no obvious signs of being non-planetary in nature; our experience with four years of *K2* data leads us to believe that most of these are indeed real planets, ready to be confirmed (e.g., via mass measurements) or statistically validated.

Table 3 lists 54 candidates that could also be transiting planets but that also include some ambiguous warning signs such as a V-shaped transit (frequently caused by eclipsing binaries). Some candidates in this list may be

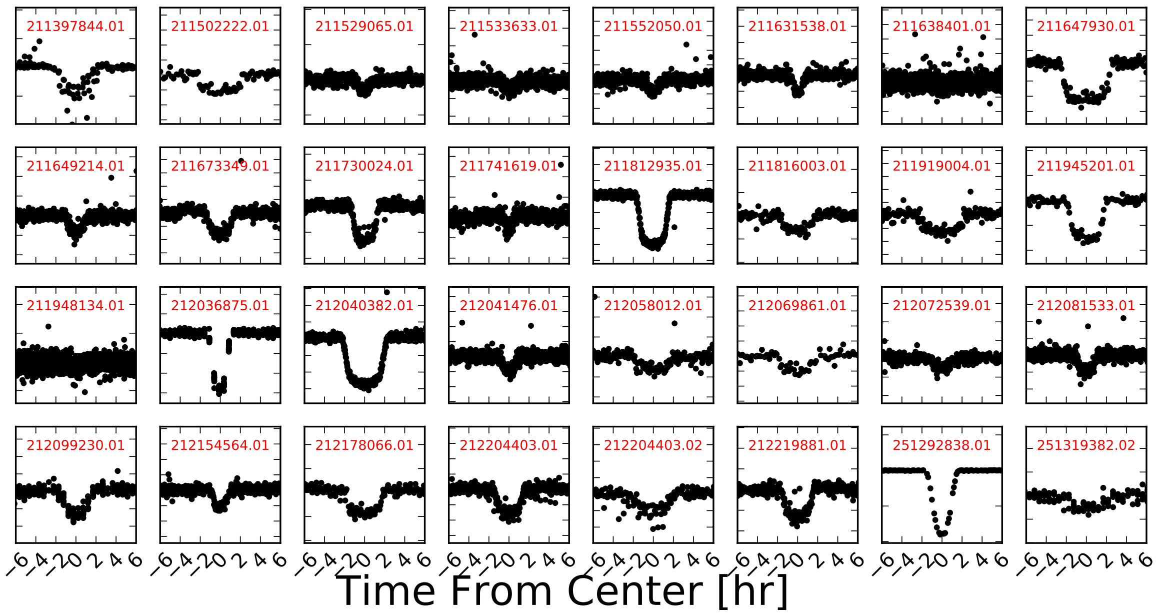

FIG. 3.— Phase-folded light curves of our 32 high-quality planet candidates. To avoid clutter, we did not label the y-axis. Their system parameters are listed in Table 2.

real planets, but many are likely non-planetary. Following the examples of the KOIs and of Vanderburg et al. (2016), we do not classify candidates with very deep transits as false positives even though transit depths $\gtrsim 5\%$ very likely indicate eclipsing binaries. We plot the light curves of these candidates in Fig. 4.

Finally, we identify a larger sample of periodic astrophysical signals that are almost certainly not caused by planets. Table 4 lists 169 targets that clearly show both transits and secondary eclipses, while Table 5 lists the 217 other periodic, astrophysical signals such as pulsation or coherent stellar rotation. There is likely overlap between these last two tables, e.g. for short-period contact/near-contact binaries whose light curves may have been classified as periodic variables.

After constructing the samples of astrophysical TCEs described above, we also perform ephemeris matching following the approach of Coughlin et al. (2014). By adopting their recommended thresholds for periods and times-of-transit, we identify a number of transit-like signals with matching ephemerides. We do not discard any of these systems, but indicate them in our target tables. This matching exercise also led us to demote 3 systems that we had originally classified as high-quality candidates (211914445.01, 211964332.01 and 251319382.01) down into a lower tier.

To provide the community access to these candidates as rapidly as possible, we have chosen to forego a full MCMC analysis on each candidate's light curve. Instead, we merely list the best-fit parameters reported by `TERRA` for each candidate in our candidate tables. In some cases `TERRA` obviously identified a multiple of the true period, and we include a note to that effect where appropriate.

4. DISCUSSION

4.1. *Host Star Parameters*

Unlike the original *Kepler* mission, *K2* does not have a homogeneous catalog of stellar parameters. Fortunately we still have the benefit of the comprehensive classification catalog of *K2* targets produced by Huber et al. (2016), who used a combination of colors, proper motions, spectroscopy, parallaxes, and galactic population synthesis models to derive stellar parameters such as effective temperatures ($T_{\rm eff}$), surface gravities ($\log g$), metallicities ([Fe/H]), radii, masses, densities, distances and extinctions for *K2* stars. The typical precision of these classifications is $\approx 2\% - 3\%$ in $T_{\rm eff}$, ≈ 0.3 dex in $\log g$ and ≈ 0.3 dex in [Fe/H] (Huber et al. 2016). We caution that the Huber et al. (2016) analysis relies on Padova stellar models (Marigo et al. 2008), which systematically underestimate the stellar radii of low-mass stars. But in the absence of spectroscopic follow-up, these are reasonable initial guesses for stellar parameters.

Fig. 5 shows the Huber et al. (2016) $T_{\rm eff}$ for the entire C16 sample, along with the distribution among our planet candidate samples. The full campaign shows three distinct populations of targets observed by *K2*, with peaks around 3500 K, 5000 K, and 6100 K. The number of candidates is of course much lower, but the distribution of $T_{\rm eff}$ for these systems appears to roughly track that of the underlying target distribution even though we do not expect it to, given the change in planet detectability as a function of stellar magnitude, radius, and noise.

In Table 2, we list the R_* and $T_{\rm eff}$ reported by Huber et al. (2016) for all of our high-quality candidates. One of these candidates, EPIC 211812935, lacks stellar parameters from Huber et al. (2016). For this star, we use the `isochrones` package[26] (Morton 2015) in conjunction with the broadband photometry for this star listed in the Ecliptic Plane Input Catalog ($BVgri$; Huber et al. 2016) to infer the stellar parameters.

4.2. *Characteristics of the Planet Candidate Sample*

[26] https://github.com/timothydmorton/isochrones

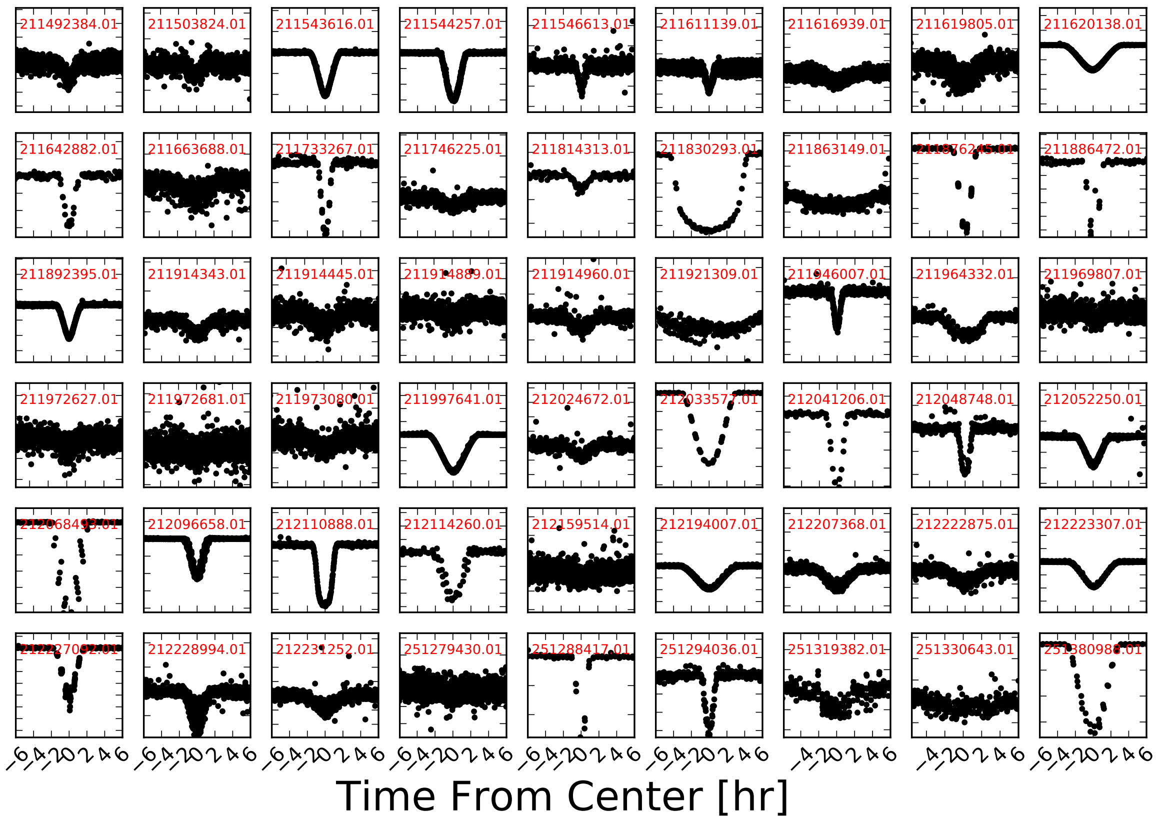

FIG. 4.— Phase-folded light curves of our 54 lower-quality planet candidates. Typical transit depths for these candidates range from 300 ppm to 700000 ppm. Their system parameters are listed in Table 3.

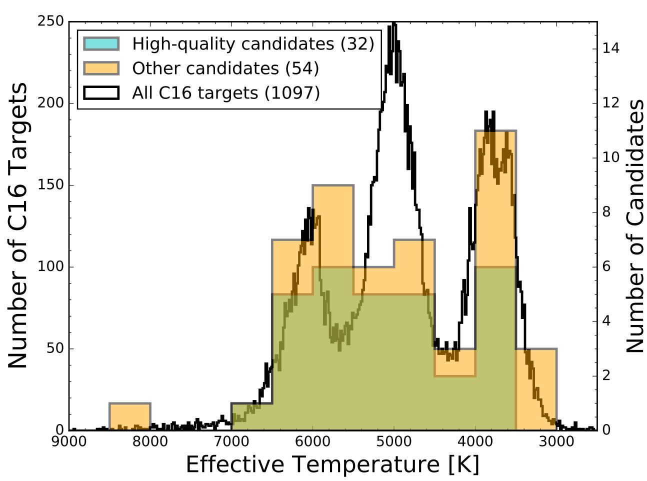

FIG. 5.— Distribution of EPIC stellar $T_{\rm eff}$ for the entire C16 target sample (empty, fine-grained histogram) and for our planet candidate sample (shaded, coarser histograms).

The period distribution of our planet candidates, along with that of the TCEs, is shown in Fig. 2. Whereas the TCE distribution peaks for $P < 1$ d, the number of high-quality candidates increases towards longer periods as expected for real planets (e.g., Fulton et al. 2017). A larger fraction of lower-quality candidates have $P < 2$ d; based on the occurrence rates of short-period planets, we expect that many of these shortest-period candidates are not planets.

Fig. 6 plots the Kepler magnitudes (Kp) and transit depths for our candidates. The highest-quality candidates orbit stars with $Kp = 10 - 15$ mag and have transit depths $\gtrsim 100$ ppm, as is typical for *K2* planet catalogs (e.g., Mayo et al. 2018). One candidate has $Kp = 6.8$ mag and is a clear outlier; this would be the brightest host star, by far, for any transiting planet discovered by *K2*. We discuss this candidate, HD 73344, in more detail in Sec. 4.3 below.

Adopting the stellar parameters of Huber et al. (2016), Fig. 7 plots the planet radius and incident irradiation of all our candidates. Two high-quality candidates have $R_P > 2R_{\rm Jup}$, but we retain these because precise stellar characterization of the host stars could plausibly result in smaller, physically realistic radii.

We detect one possible multi-planet system, with two high-quality candidates around EPIC 212204403. These have periods of 4.7 and 12.6 d and sizes of approximately 3.3 and 2.6 $R_\oplus$, respectively. Based on past studies of multi-planet systems these candidates are likely to be real planets (Lissauer et al. 2012; Sinukoff et al. 2016). Validating them is beyond the scope of this work, but at $V = 12.564$ mag, the system could be an interesting target for radial velocity (RV) mass measurements of multi-planet systems.

Another interesting candidate is EPIC 212048748.01 from the lower-quality "plausible planet candidate" list.

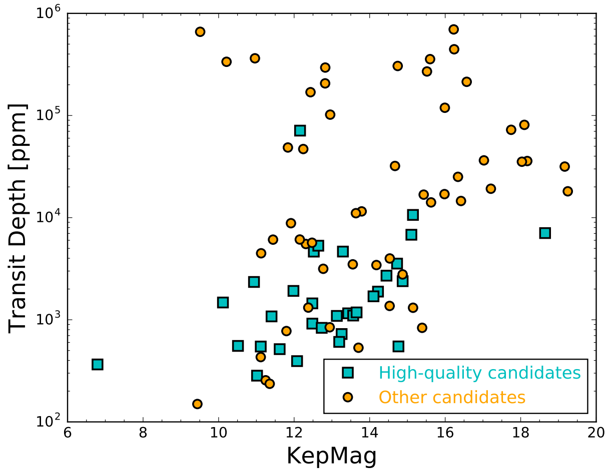

FIG. 6.— Transit depth and stellar magnitude for our planet candidates.

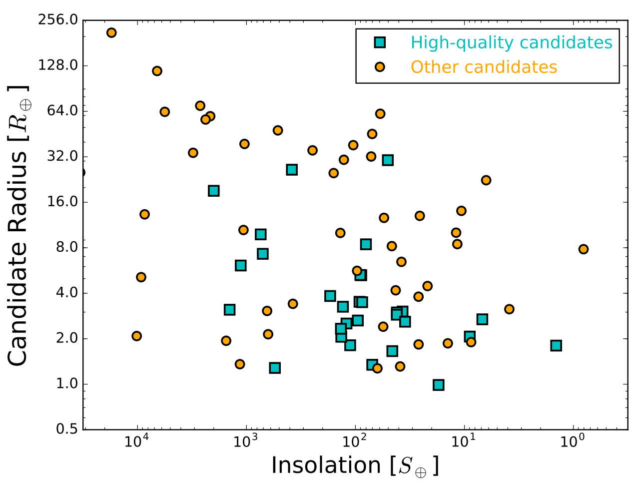

FIG. 7.— Approximate radii and incident insolation for our high-quality candidates (light blue squares) lower-quality candidates (orange circles).

This candidate transits with a 3155 ppm depth and a period of 5.75 d around a high proper motion, infrared bright ($K = 9.2$) star having optical-IR photometry consistent with an M3 spectral type. If confirmed, this $\sim 2R_\oplus$ candidate will be a priority target for upcoming IR sensitive precision RV instruments and transit spectroscopy with the James Webb Space Telescope.

Finally, a comparison with the NASA Exoplanet Archive shows that four of our candidates have already been validated using data from C5. Dressing et al. (2017) validated two of our high-quality C16 candidates, 212069861.01 (K2-123b) and 212154564.01 (K2-124b); another candidate 212110888.01 is a previously known hot Jupiter K2-34b (Lillo-Box et al. 2016; Hirano et al. 2016); and our lower-priority candidate 211969807.01 was validated as K2-104b (Mann et al. 2017). Our derived system parameters are in approximate agreement with those in the discovery papers. A combined analysis of the C5 and C16 data (possible for many targets in C16) may prove fruitful for these systems.

4.3. *HD 73344*

One candidate of particular interest is HD 73344[27] (HIP 42403, EPIC 212178066), whose light curve is shown in Fig 1. This bright F star ($V = 6.9$ mag) is highly saturated in the *K2* data, but a custom aperture encompassing the entire saturated PSF shows the clear transit-like signal highlighted in Fig. 1. Although our purpose is to quickly present candidates to the community, we pause here to briefly investigate this intriguing signal.

The star has been characterized by many groups over the years (e.g., Valenti & Fischer 2005; Paletou et al. 2015), indicating that it lies at a distance of 35.0 ± 0.5 pc (Gaia Collab. et al. 2016) and its parameters are $T_{\rm eff} = 6120 \pm 50$ K, $R_* = 1.15 \pm 0.04\,R_\odot$, $M_* = 1.26 \pm 0.19\,M_\odot$. The star's projected rotational velocity is $v \sin i = 6.3 \pm 0.5$ km s^{-1} (Valenti & Fischer 2005), and our light curve shows evidence of stellar rotation at a period (determined via Lomb-Scargle periodogram) of 8.5 ± 0.5 d. This period would be consistent with the rotation periods of other stars with similar colors, and is consistent with a stellar age of roughly 1 Gyr (Angus et al. 2015). Combining all these parameters indicates that the stellar rotation axis is inclined by $i = 62^\circ \pm 10^\circ$. Thus, if the candidate signal comes from an object orbiting HD 73344, the angular momentum of the star and the transiting object's orbit are likely misaligned.

Because the star is strongly saturated, we cannot apply a standard centroid analysis of the stellar position in- vs. out-of-transit. However, a transit analysis (identical to that described by Crossfield et al. 2015) implies a stellar density of $\rho_{*,circ} = 2.2 \pm 1.2$ g cm^{-3} — a loose constraint, but consistent with the spectroscopically-inferred stellar density of 1.2 ± 0.2 g cm^{-3} and much higher than the low stellar densities that might be expected from an eclipsed giant star. The results of our transit analysis, which includes dilution as a free parameter, are also consistent with no dilution.

The resulting parameters from our transit analysis of HD 73344 are listed in Table 1. If the transits are occurring around the target and not around a background star in the photometric aperture, the stellar radius and transit depth imply a candidate radius of roughly 2.6 $R_\oplus$. This size would imply a corresponding candidate mass of $10 \pm 3\,M_\oplus$ (Wolfgang et al. 2016) and an RV amplitude of $\sim$2 m s^{-1}. The star was observed 24 times over eleven years as part of the Lick radial velocity survey (Fischer et al. 2014), but these data have an RMS of 32 m s^{-1} (despite internal uncertainties of roughly 6 m s^{-1}) and show no coherent RV signal at the candidate period or at our calculated stellar rotation period. Nightly Keck/HIRES RVs over four consecutive nights in 1999 showed a stellar jitter of 3.9 m s^{-1} (Isaacson & Fischer 2010). HD 73344 also exhibits moderate chromospheric activity ($S_{HK} = 0.22$, $R'_{HK} = -4.66$; Isaacson & Fischer 2010), but at this $T_{\rm eff}$ H&K activity is not the main contribution to jitter. It seems likely that precise

[27] This target was proposed by many K2 GO programs: 16009 (PI Charbonneau), 16010 (PI Lund), 16021 (PI Howard), 16028 (PI Cochran), 16063 (PI Redfield), 16068 (PI Jensen), and 16081 (PI Guzik)

TABLE 1
Candidate Parameters for HD 73344

Parameter	Units	Value
T_0	$\mathrm{BJD_{TDB}} - 2454833$	$3262.8931^{+0.0020}_{-0.0023}$
P	d	$15.61335^{+0.00085}_{-0.00078}$
i	deg	$89.15^{+0.61}_{-1.13}$
R_{circ}/R_*	%	$2.04^{+0.15}_{-0.10}$
T_{14}	hr	$3.46^{+0.20}_{-0.17}$
T_{23}	hr	$3.22^{+0.21}_{-0.18}$
R_*/a	–	$0.0327^{+0.0118}_{-0.0042}$
b	–	0.46 ± 0.32
$\rho_{*,\mathrm{circ}}$	g cm^{-3}	$2.2^{+1.1}_{-1.3}$
a	AU	$0.1321^{+0.0063}_{-0.0070}$
R_{cand}	R_E	2.56 ± 0.18
S_{inc}	S_E	96^{+12}_{-11}

RV measurements could confirm this planet candidate — perhaps even before it sets for the season in May-June 2018.

4.4. *Conclusions*

In a short timespan, we have converted cadence-level *K2* data into time-series photometry of 20647 targets, identified 1097 periodic signals (of astrophysical or instrumental origin), and distilled these into 32 high-quality planet candidates, 54 lower-quality candidates, 169 eclipsing binaries, and 217 other periodically-variable astrophysical sources. Four of our candidates have already been validated as planets (see Sec. 4.2), suggesting that our approach successfully identifies planet-like signals. One particularly interesting new target is HD 73344, a $V = 6.9$ F dwarf which may host a 2.6 $R_\oplus$ planet on a 15 d orbit (see Sec. 4.3). We have released parameters for all identified systems of interest, along with light curves and transit vetting plots[28], in the belief that rapid identification and public dissemination of interesting signals will maximize the scientific productivity of *K2*. If *K2* continues operating through the end of C17 (another forward-facing campaign), it may prove useful to perform a similarly rapid analysis of those data.

This rapid-release model is also somewhat of an analog for the upcoming *TESS* mission (Ricker et al. 2014). The release of planet catalogs has occurred only irregularly during the *K2* mission, but this paradigm will change once *TESS* operations begin in earnest. Data from *TESS* will be released and processed on a 27-day rhythm for most of the two-year mission duration. With the shorter observing windows, ephemeris decay is also a much larger problem for *TESS* and therefore the importance of securing planet candidates in the same season is even higher. If interesting objects could be rapidly gleaned from *TESS* data and circulated to the community, follow-up observations and analyses could begin a full season earlier and so the full impact of that mission could more quickly be achieved.

[28] All available soon/now at `https://exofop.ipac.caltech.edu/k2/`, or by request.

We thank all those who selected the targets observed in C16. I.J.M.C. acknowledges support from NASA through K2GO grant 80NSSC18K0308 and from NSF through grant AST-1824644. He also gratefully acknowledges the hospitality of the organizers and participants of the "Challenge to Super-Earths" workshop at NAOJ, during which much of this work took place. This research has made use of the Exoplanet Follow-up Observing Program (ExoFOP), which is operated by the California Institute of Technology, under contract with the National Aeronautics and Space Administration.

Facilities: Kepler, K2

REFERENCES

Angus, R., Aigrain, S., Foreman-Mackey, D., & McQuillan, A. 2015, MNRAS, 450, 1787, ADS, 1502.06965
Barentsen, Geert; Cardoso, J. V. d. M. 2018, Kadenza: Kepler/K2 Raw Cadence Data Reader, Astrophysics Source Code Library, ADS
Christiansen, J. L. et al. 2018, AJ, 155, 57, ADS, 1801.03874
Coughlin, J. L. et al. 2014, AJ, 147, 119, ADS, 1401.1240
Crossfield, I. J. M. et al. 2016, ApJS, 226, 7, ADS, 1607.05263
—. 2015, ApJ, 804, 10, ADS, 1501.03798
Dressing, C. D. et al. 2017, AJ, 154, 207, ADS, 1703.07416
Fischer, D. A., Marcy, G. W., & Spronck, J. F. P. 2014, ApJS, 210, 5, ADS, 1310.7315
Fulton, B. J. et al. 2017, AJ, 154, 109, ADS, 1703.10375
Gaia Collab. et al. 2016, A&A, 595, A2, ADS, 1609.04172
Hirano, T. et al. 2016, ApJ, 825, 53, ADS, 1602.00638
Howell, S. B. et al. 2014, PASP, 126, 398, ADS, 1402.5163
Huber, D. et al. 2016, ApJS, 224, 2, ADS, 1512.02643
Isaacson, H., & Fischer, D. 2010, ApJ, 725, 875, ADS, 1009.2301
Lillo-Box, J. et al. 2016, A&A, 594, A50, ADS, 1601.07635
Lissauer, J. J. et al. 2012, ApJ, 750, 112, ADS, 1201.5424
Mandel, K., & Agol, E. 2002, ApJ, 580, L171, ADS, astro-ph/0210099
Mann, A. W. et al. 2017, AJ, 153, 64, ADS, 1609.00726
Marigo, P., Girardi, L., Bressan, A., Groenewegen, M. A. T., Silva, L., & Granato, G. L. 2008, A&A, 482, 883, ADS, 0711.4922
Mayo, A. W. et al. 2018, ArXiv e-prints, ADS, 1802.05277
Morton, T. D. 2015, isochrones: Stellar model grid package, Astrophysics Source Code Library, 1503.010, ADS
Oelkers, R. J. et al. 2018, AJ, 155, 39, ADS, 1711.03608
Paletou, F., Böhm, T., Watson, V., & Trouilhet, J.-F. 2015, A&A, 573, A67, ADS, 1411.4859
Petigura, E. A. et al. 2018, AJ, 155, 21, ADS, 1711.06377
Petigura, E. A., Howard, A. W., & Marcy, G. W. 2013a, Proceedings of the National Academy of Science, 110, 19273, ADS, 1311.6806
Petigura, E. A., Marcy, G. W., & Howard, A. W. 2013b, ApJ, 770, 69, ADS, 1304.0460
Petigura, E. A. et al. 2015, ApJ, 811, 102, ADS, 1507.08256
Ricker, G. R. et al. 2014, in Society of Photo-Optical Instrumentation Engineers (SPIE) Conference Series, Vol. 9143, Society of Photo-Optical Instrumentation Engineers (SPIE) Conference Series, 20, 1406.0151, ADS
Sinukoff, E. et al. 2016, ApJ, 827, 78, ADS, 1511.09213
Thompson, S. E. et al. 2017, ArXiv e-prints, ADS, 1710.06758
Valenti, J. A., & Fischer, D. A. 2005, ApJS, 159, 141, ADS
Vanderburg, A., & Johnson, J. A. 2014, PASP, 126, 948, ADS, 1408.3853
Vanderburg, A. et al. 2016, ApJS, 222, 14, ADS, 1511.07820
Wolfgang, A., Rogers, L. A., & Ford, E. B. 2016, ApJ, 825, 19, ADS, 1504.07557

TABLE 2
High-quality candidate parameters

Candidate	Kp	P [d]	T_0 [BJD - 2454833]	T_{14} [d]	$(R_P/R_*)^2$ [ppm]	R_* [$R_\odot$]	$T_{\rm eff}$ [K]	R_P [$R_\oplus$]	$S_{\rm inc}$ [$F_\oplus$]	Comment
211397844.01	13.292	16.166729	3274.81627	0.1331	4653	3.5	4937	26.3	383	—
211502222.01	11.617	22.996469	3280.30463	0.1550	515	1.4	6110	3.5	91	—
211529065.01	13.431	4.399372	3264.74269	0.0532	1156	0.7	4701	2.6	95	—
211533633.01	13.258	2.127017	3262.65841	0.0590	724	0.5	3992	1.3	70	—
211552050.01	13.194	3.545471	3264.94603	0.0610	607	0.7	4639	1.8	111	—
211631538.01	14.221	5.513105	3266.24807	0.0386	1886	0.7	4885	3.5	86	—
211638401.01	14.763	0.530219	3262.64715	0.0443	548	0.5	4067	1.3	548	—
211647930.01	11.982	14.759545	3264.39384	0.1712	1916	1.1	5846	5.3	90	—
211649214.01	14.726	3.787955	3265.41865	0.0688	3547	2.9	4993	19.0	1996	—
211673349.01	14.446	4.894435	3264.62717	0.0877	2702	0.5	4245	3.0	36	—
211730024.01	11.402	5.113776	3263.81006	0.0896	1078	1.7	6506	6.1	1129	—
211741619.01	13.564	2.787624	3263.82245	0.0311	1099	0.5	3919	1.7	45	—
211812935.01[a]	12.640	3.608008	3264.87916	0.1141	5310	1.9	7348	15.5	3345	—
211816003.01	13.654	14.455276	3265.78864	0.1140	1180	0.8	5434	3.0	41	—
211919004.01	13.131	11.722909	3265.36631	0.1546	1090	0.8	5086	2.9	41	—
211945201.01	10.115	19.492036	3280.93977	0.1240	1475	1.3	6084	5.3	88	—
212036875.01	10.937	5.170131	3265.68053	0.0646	2345	1.4	6336	7.3	708	—
212040382.01	12.521	4.445545	3266.34920	0.1513	4648	1.3	6123	9.8	740	—
212041476.01	12.078	2.783774	3262.55678	0.0530	393	1.4	5962	3.1	1427	—
212058012.01	11.018	11.560844	3266.11106	0.1281	283	1.1	5903	2.1	134	—
212069861.01	14.102	30.955010	3274.10951	0.1368	1696	0.4	3839	1.8	1.41	K2-123b (Dressing et al. 2017)
212072539.01	14.874	7.677182	3263.56943	0.0733	2385	0.4	3857	2.1	8.9	—
212081533.01	12.731	3.355780	3262.74776	0.0635	833	0.3	3679	1.0	17	—
212099230.01	10.513	7.111692	3269.13864	0.1046	554	0.9	5537	2.3	135	—
212110888.01	11.441	2.995626	3263.95812	0.0813	6090	1.2	6093	10.5	1065	K2-34b (Lillo-Box et al. 2016; Hirano et al. 2016)
212154564.01	15.105	6.414024	3264.81441	0.0699	6800	0.3	3643	2.7	6.9	K2-124b (Dressing et al. 2017)
212178066.01	6.793	15.615671	3262.88899	0.1256	365	1.2	6120	2.6	96	HD 73344
212204403.01	12.482	4.688771	3263.71227	0.0964	1446	0.8	5025	3.3	130	possible multi
212204403.02	12.482	12.554007	3271.42578	0.1179	917	0.8	5025	2.6	35	possible multi
212219881.01	15.147	6.924813	3264.18565	0.1189	10630	0.8	5106	8.4	80	—
251292838.01	12.157	19.581960	3274.28574	0.1132	71135	1.0	5704	30.4	50	—
251319382.02[b]	11.116	14.877227	3270.59086	0.1193	547	1.5	5966	3.8	170	—

[a] Parameters not in EPIC; classified using `isochrones` as described in Sec. 4.1.
[b] Possible multi, but the ephemeris of 251319382.01 matches that of another TCE (see Table 3). We identified hints of a third candidate in this system, with a period of ~ 3.5 d and S/N$\sim$7.

TABLE 3
PLAUSIBLE CANDIDATE PARAMETERS

Candidate	Kp	P [d]	T_0 [BJD - 2454833]	T_{14} [d]	$(R_P/R_*)^2$ [ppm]	Comment	Ephemeris matching
211492384.01	12.375	0.635388	3262.97292	0.0543	1315	somewhat V-shaped	
211503824.01	11.246	2.047321	3263.17683	0.0789	255	slightly asymmetric	
211543616.01	15.600	1.518233	3263.37665	0.1284	356389	V-shaped	
211544257.01	12.242	1.630244	3263.44772	0.0952	46964	somewhat V-shaped; spotted star?	
211546613.01	15.982	2.007583	3263.89131	0.0377	16989	V-shaped	
211611139.01	12.474	1.882271	3263.60192	0.0402	5678	somewhat V-shaped	
211616939.01	11.796	1.856025	3262.61010	0.1167	775	V-shaped	251404897.01, 212041206.01
211619805.01	12.942	1.855352	3262.61816	0.1257	844	somewhat V-shaped	211948134.01, 212041206.01
211620138.01	9.512	1.855381	3262.62283	0.2368	660084	V-shaped	
211642882.01	13.788	23.899013	3267.90219	0.0618	11511	V-shaped	211948134.01, 251404897.01
211663688.01	16.419	1.856025	3262.60227	0.1698	14554	V-shaped	
211733267.01	12.150	8.657873	3264.31999	0.0410	6106	slightly V-shaped	
211746225.01	19.166	2.131475	3263.40635	0.1439	31623	somewhat V-shaped	211621644.01
211814313.01	15.431	15.404424	3265.31020	0.1172	16796	V-shaped	
211830293.01	11.916	20.893387	3281.64951	0.3209	8821	possible eclipse at phase 0.53	
211863149.01	14.873	2.612926	3264.30868	0.2776	2779	V-shaped	251374534.02, 251384067.01
211876245.01	15.518	8.971461	3266.46238	0.1086	269917	Somewhat V-shaped; hint of eclipse	
211886472.01	11.126	19.639079	3281.74811	0.0591	4477	V-shaped	
211892395.01	16.238	0.995060	3262.63726	0.1102	445224	V-shaped	
211914343.01	17.210	1.810878	3263.47001	0.1166	19184	somewhat V-shaped	211816003.01, 211914960.01, 212020442.01, 251809628.01
211914445.01	14.529	1.810343	3263.47930	0.1002	1366	—	212020442.01, 251809286.01, 251809628.01
211914889.01	18.032	1.810529	3263.47752	0.1544	35275	somewhat V-shaped	211816003.01, 212020442.01, 251809286.01
211914960.01	14.179	1.811362	3263.45752	0.1185	3433	V-shaped	211816003.01, 211914343.01, 212020442.01, 251809628.01
211921309.01	17.026	9.477889	3264.54207	0.5575	36370	noisy – possibly variable depth	
211946007.01	16.570	1.982808	3263.85033	0.0568	213762	somewhat V-shaped	
211948134.01	18.646	0.501684	3262.47050	0.0357	7060	somewhat V-shaped.	
211964332.01	14.533	7.220291	3266.50297	0.1714	3983	—	211644647.01, 211849962.01, 211852187.01, 25138775.01
211964555.01	18.314	7.220943	3266.50089	0.2204	34668	somewhat V-shaped	
211969807.01	15.149	1.974960	3262.86635	0.0705	1310	K2-104b (Mann et al. 2017); marginal detection.	
211972627.01	11.353	1.092707	3263.46288	0.0677	236	V-shaped	
211972681.01	15.390	1.092810	3263.45999	0.0544	833	V-shaped (or short transit duration)	211858408.01, 251315031.01, 211402878.02
211973080.01	16.339	1.093008	3263.45048	0.1222	25085	likely SE; somewhat V-shaped	251319382.01, 211858408.01, 211402878.02
211997641.01	12.821	1.744596	3263.51457	0.1635	206372	v-shaped	
212024672.01	18.174	3.696095	3262.88391	0.1397	35827	slightly V-shaped; hint of eclipse	211885185.01
212033577.01	11.835	23.702338	3285.09369	0.2260	48619	V-shaped	
212041206.01	14.671	23.918833	3283.38350	0.0717	32061	V-shaped	
212048748.01	12.771	5.745780	3262.55747	0.0472	3155	V-shaped	
212052250.01	14.743	0.986768	3262.87574	0.1390	305455	V-shaped – likely even-odd	
212068493.01	12.955	14.226672	3271.78105	0.1452	101983	V-shaped	
212096658.01	10.210	1.466477	3263.68203	0.1062	335755	V-shaped	
212114260.01	12.311	20.009593	3265.55763	0.1006	5520	likely eclipse	
212159514.01	13.704	0.545641	3262.55097	0.0798	532	somewhat asymmetric	
212194007.01	12.824	1.177176	3262.94296	0.1635	294749	V-shaped	
212207368.01	15.626	1.190338	3263.29145	0.1358	14098	V-shaped	211611139.01, 211619805.01, 211914343.01
212222875.01	18.097	1.190021	3263.30080	0.1779	80984	V-shaped, spatially coincides with 212231252	212231252.01
212223307.01	10.962	1.190358	3263.28896	0.1635	363154	V-shaped	
212227092.01	16.226	5.190251	3266.42852	0.1317	696741	V-shaped	
212228994.01	13.553	1.095850	3263.34696	0.0796	3489	V-shaped; variable depth	
212231252.01	17.747	1.190361	3263.29044	0.1636	72434	V-shaped, coincides with 212222875	212222875.01
251279430.01	9.438	0.719634	3262.56083	0.0639	149	somewhat V-shaped	
251288417.01	15.991	20.925208	3279.57571	0.0639	119088	V-shaped	
251294036.01	13.636	6.855567	3268.72849	0.0526	11053	somewhat V-shaped	
251319382.01	11.116	8.235945	3265.71902	0.1293	430	V-shaped	
251330643.01	19.247	5.997279	3265.29262	0.3287	18101	—	212012387.01

TABLE 3 — *Continued*

Candidate	Kp	P [d]	T_0 [BJD - 2454833]	T_{14} [d]	$(R_P/R_*)^2$ [ppm]	Comment	Ephemeris matching
251380988.01	12.434	30.920978	3274.20733	0.2285	169142	slightly V-shaped	

TABLE 4
SYSTEMS WITH SECONDARY ECLIPSES

Candidate	Kp	P [d]	T_0 [BJD$_{TDB}$ - 2454833]	T_{14} [d]	$(R_P/R_*)^2$ [ppm]	Comment	Ephemeris matching
211397774.01	15.649	0.967865	3262.83095	0.1047	149235	even-odd – half-period	
211402878.01	14.498	25.236580	3277.84155	0.1427	131088		
211408138.01	12.740	10.337864	3267.82296	0.2954	50598		
211409299.01	11.951	13.919301	3263.16370	0.2036	126507		
211411891.01	12.776	0.954863	3262.53608	0.0928	122533		
211422822.01	15.664	0.554633	3262.67870	0.0547	26770		
211425822.01	14.888	2.153178	3263.18086	0.1114	161675		
211429934.01	14.147	0.565934	3262.47647	0.0817	76907		
211430148.01	14.892	15.091257	3262.98697	0.1731	387212		
211431013.01	14.738	3.102398	3265.15784	0.2575	116056	even-odd – half-period	
211432167.01	8.550	5.817737	3263.03384	0.1202	9442		212048503.01
211432176.01	9.866	5.817854	3263.03296	0.1200	9632		211914718.01
211432946.01	14.398	1.671965	3263.07264	0.0897	321572	even-odd – half-period	
211449931.01	14.659	6.663685	3262.53719	0.1092	77241		
211452175.01	12.406	11.114394	3268.75989	0.2596	140535		
211453076.01	16.341	0.524461	3262.66075	0.0714	8800	twice period	
211453223.01	14.590	9.056947	3264.66347	0.1389	228283		
211468153.01	14.381	0.737735	3262.69611	0.0817	293171		
211471048.01	12.867	0.799768	3262.64738	0.1499	368062		
211477347.01	15.368	1.641114	3263.39459	0.1835	232835		
211490299.01	15.991	0.555516	3262.88867	0.0616	125677		
211492541.01	12.789	1.031746	3262.80400	0.2313	13062		
211493669.01	12.976	0.583370	3262.72350	0.0485	16936		
211509665.01	16.519	3.247194	3263.55605	0.1960	274993	even-odd – half-period	
211524114.01	11.473	0.715676	3262.65638	0.0520	1668		
211524558.01	14.161	0.546969	3262.99346	0.0817	496880	twice period	
211526186.01	12.814	0.682618	3262.60560	0.0487	10943	even-odd – 1.5× period	
211534342.01	15.873	0.512702	3262.52406	0.0751	259506		
211535481.01	14.979	0.539696	3262.52362	0.0727	101331	V-shaped; likely even-odd	
211538193.01	13.908	0.597258	3262.98601	0.0817	250566		
211540348.01	14.022	0.620388	3262.73962	0.0817	497678		
211563123.01	12.583	17.325857	3265.30498	0.3548	334820		
211589784.01	12.678	1.359386	3263.68715	0.0767	92013		
211600389.01	14.157	0.630717	3263.02647	0.0817	163414		211449931.01
211600632.01	16.688	0.630718	3263.02663	0.0817	164032		211432176.01
211604981.01	12.727	12.427163	3267.32649	0.2241	16631		
211607670.01	12.793	1.348851	3263.01356	0.1584	217820	even-odd – half-period	
211607804.01	13.358	1.490219	3263.43270	0.1635	733825		
211613886.01	12.729	0.958786	3263.10671	0.0522	17691		
211619120.01	13.059	11.100314	3264.29172	0.5242	123582		
211621644.01	15.443	0.921358	3262.74784	0.0694	127918	thrice period	
211621961.01	16.548	11.078847	3265.06284	0.5970	121654		
211625003.01	12.848	0.530431	3262.92711	0.0817	409431	even-odd; 1.5× period	
211626490.01	12.886	0.747734	3262.90935	0.0817	287143		
211630537.01	14.185	0.697190	3262.80305	0.0773	34039		
211631904.01	13.989	0.884004	3262.66371	0.0882	391961		
211638883.01	12.622	0.543877	3262.47515	0.0282	659		
211639283.01	15.088	6.741846	3266.59522	0.3020	55296	slightly V-shaped	
211644647.01	13.304	2.044175	3264.21457	0.2978	71960	even-odd – half-period	
211651743.01	13.962	0.516235	3262.68635	0.0817	111574		
211662047.01	14.791	0.635238	3262.94146	0.0637	126462		
211663508.01	14.343	0.544418	3262.51405	0.0813	434869	four times period	
211664543.01	15.812	0.698333	3262.97188	0.0550	106429	thrice period	
211710534.01	12.203	3.022569	3263.74324	0.1410	56458		
211718105.01	14.103	2.958763	3264.20177	0.2411	176980	even-odd – half-period	

TABLE 4 — *Continued*

Candidate	Kp	P [d]	T_0 [BJD$_{TDB}$ - 2454833]	T_{14} [d]	$(R_P/R_*)^2$ [ppm]	Comment	Ephemeris matching
211721325.01	15.428	1.052364	3262.72164	0.1179	348537		
211732801.01	10.655	2.131554	3263.40544	0.1694	68562	V-shaped; even-odd – half-period	251411166.01
211737652.01	16.354	2.468190	3262.93777	0.2452	483890		
211738534.01	15.604	0.568020	3262.64187	0.1389	13803		
211744153.01	14.861	4.612166	3265.94990	0.0664	5543		
211750072.01	13.005	0.595558	3263.09743	0.0705	51711		
211759163.01	14.804	0.595667	3262.90859	0.0620	129607	five times period	
211764271.01	12.895	3.576744	3262.91264	0.1222	68508		211431013.01
211764373.01	11.409	3.576780	3262.91248	0.1111	31467	likely SE	211607804.01
211768007.01	14.021	0.542912	3262.56186	0.0748	120270	twice period	
211770390.01	12.239	3.790180	3262.68640	0.2469	52183	even-odd – half-period	
211807456.01	14.973	0.504961	3262.86244	0.0756	291504	twice period	
211809568.01	15.456	0.593274	3262.99164	0.0817	636988	twice period	
211812160.01	13.485	1.085097	3262.91626	0.0898	31653		
211814733.01	11.971	14.707213	3268.97802	0.0892	4206		
211822953.01	16.834	1.549381	3262.83336	0.0684	92689		
211828142.01	17.558	20.180269	3268.57729	0.1192	395334		
211829982.01	13.823	5.803439	3264.34997	0.1628	627831		
211838158.01	15.801	0.575349	3262.87166	0.0817	522455	twice period	
211839430.01	10.730	2.612938	3264.30391	0.3813	114984	even-odd – half-period	251384067.01, 212048748.01
211839462.01	10.037	2.612804	3264.30654	0.3681	91385	even-odd – half-period	251374534.02, 212048748.01
211841496.01	15.486	0.522199	3262.46826	0.0676	35912		
211852187.01	17.636	14.343042	3266.06818	0.0610	110696		
211858408.01	12.427	0.628876	3262.79149	0.0817	109867		
211858489.01	12.270	0.636109	3262.49271	0.0290	1465		
211885185.01	12.493	4.397187	3262.92467	0.2452	203447		
211906940.01	16.368	0.526316	3262.47776	0.0418	364733	thrice period	
211910237.01	14.750	1.108972	3263.36936	0.0760	37369	odd-even – half-period	
211914718.01	11.448	0.582017	3262.66714	0.0817	376942	twice period	
211915147.01	9.023	1.810708	3263.47340	0.1267	35675	odd-even; half-period	211816003.01, 251809286.01, 251809628.01
211919555.01	16.889	9.484994	3264.50601	0.6098	82338		211764271.01, 211812160.01, 228682364.01
211919842.01	15.625	9.510911	3264.32358	0.4087	7834		
211920462.01	19.874	9.516793	3264.29495	0.4087	408803		
211920528.01	12.279	9.486580	3264.50407	0.4341	2153		211738534.01, 211812160.01, 228682364.01
211920604.01	12.258	9.487929	3264.49219	0.5031	8783		211738534.01, 211764271.01, 228682364.01
211920811.01	12.482	9.492590	3264.47004	0.4525	4713		
211928959.01	16.703	0.858462	3263.16644	0.0845	248568		
211934173.01	18.229	0.520451	3262.60163	0.0259	34196		
211942157.01	12.051	1.324292	3263.37798	0.2452	249317		
211955798.01	14.902	0.616444	3263.06087	0.0290	5674	thrice period	
211964001.01	9.402	7.218071	3266.51847	0.1993	32035		211644647.01, 211852187.01, 251308775.01, 2513...
211964025.01	7.605	7.219626	3266.50648	0.2035	31796		211644647.01, 211849962.01, 251308775.01, 2513...
211964555.01	18.314	7.220943	3266.50089	0.2204	34667		211849962.01, 211852187.01, 251308775.01, 2513...
211972837.01	13.547	1.092917	3263.45491	0.1566	1355446		251319382.01, 251315031.01, 211402878.02
212009702.01	13.173	0.923861	3263.37075	0.1382	345965		
212010565.01	14.531	2.851451	3263.72690	0.3877	992969		
212012387.01	13.972	3.244126	3264.32148	0.1609	405896	even-odd – half-period	
212019055.01	12.700	0.821436	3263.14571	0.0991	162008		
212020442.01	13.974	3.888853	3263.60805	0.1295	25872	even-odd – half-period	
212024647.01	10.279	3.696871	3262.87322	0.1286	124336		251383916.01
212026226.01	16.843	1.769505	3263.39804	0.1512	176962	even-odd – half-period	
212037403.01	13.231	3.408190	3265.44045	0.1191	164327		
212039539.01	11.647	2.229820	3263.61073	0.2225	247831		
212044495.01	12.733	1.830767	3263.40493	0.1187	157032		
212048503.01	13.625	0.617674	3262.65639	0.0817	598171	twice period	
212053988.01	15.028	0.579309	3262.53528	0.0817	471689	twice period	

TABLE 4 — *Continued*

Candidate	Kp	P [d]	T_0 [BJD$_{TDB}$ - 2454833]	T_{14} [d]	$(R_P/R_*)^2$ [ppm]	Comment	Ephemeris matching
212060710.01	14.273	1.204338	3262.76086	0.1057	406463		
212060895.01	16.782	0.604228	3262.94672	0.0704	196260	twice period	
212066805.01	10.410	0.816734	3262.60536	0.0505	5075		
212069706.01	14.410	0.547674	3262.88638	0.0239	1629	twice-period	
212071939.01	13.598	1.743013	3262.49990	0.2452	470271		
212075294.01	15.873	0.550820	3262.88533	0.0789	319979	twice period	
212075842.01	14.516	1.153456	3262.92758	0.2072	128377	possible even-odd	
212082682.01	14.611	3.797473	3262.81109	0.1082	118402		
212083250.01	11.967	0.518748	3262.97005	0.0817	157737		211934173.04
212083455.01	12.262	0.518754	3262.96851	0.0344	228		211934173.03
212085654.01	13.900	0.989720	3262.87427	0.1128	168919		
212085740.01	13.688	4.845561	3263.15766	0.1162	77469		
212086717.01	14.757	0.643142	3263.04961	0.0817	450377	twice period	
212109233.01	12.624	1.991357	3262.74598	0.1259	96349		
212110007.01	14.245	16.709659	3264.12649	0.1373	112830		
212115388.01	14.605	1.488249	3262.99356	0.0756	48367	even-odd – half-period	
212116340.01	12.079	0.610205	3262.87662	0.0817	136330		212009702.01
212117087.01	12.245	1.076390	3262.97882	0.1212	91275	even-odd – half-period	
212154158.01	12.300	1.023613	3263.35564	0.2126	11010		
212163353.01	13.539	5.173531	3265.85411	0.1336	58580		
212171851.01	14.143	5.489456	3266.59388	0.5965	370025		
212175087.01	13.431	0.699705	3262.85587	0.1975	244959		
212181307.01	15.502	0.555317	3262.74524	0.0817	416594	twice period	
212181460.01	14.620	0.569192	3262.70026	0.0817	276502		
212182233.01	14.991	0.751394	3262.93405	0.0817	628169		
212207194.01	12.285	9.148701	3265.32727	0.2275	119700		
212208163.01	15.437	2.724469	3263.01388	0.2452	665629		
212210390.01	13.136	12.886147	3262.90925	0.1161	62814		
212214592.01	13.803	0.723102	3263.08482	0.0820	58108		
212221986.01	15.093	0.526018	3262.72081	0.0597	236909		
212225413.01	13.937	0.793048	3263.13909	0.1360	200400		
212225806.01	15.251	0.594392	3262.90962	0.0817	406214	double period	
212225986.01	13.668	1.160308	3263.03616	0.0993	205206	even-odd – half-period	
212228588.01	14.794	0.598120	3262.85185	0.0606	108294		211759163.01
228682364.01	19.970	0.872893	3263.15278	0.1432	68394		
251281013.01	14.183	3.287912	3265.59014	0.1247	107725	even-odd – half-period	
251286992.01	15.448	0.505602	3262.78219	0.0740	410848	twice period	
251292508.01	15.238	1.288312	3263.63014	0.0829	241729	even-odd – half-period	
251307609.01	15.183	0.598197	3262.86830	0.0817	379663	twice period	212085740.01
251308775.01	11.989	2.804246	3263.72840	0.1635	69100		
251314585.01	14.440	0.691617	3263.02339	0.0817	98244		
251315031.01	13.537	0.540527	3262.97430	0.0788	333734		
251327548.01	11.636	11.349445	3268.62400	0.2443	59759		
251330444.01	11.202	5.998652	3265.28349	0.4500	83190	odd-even – half-period.	251319382.02
251345848.01	12.505	2.883162	3263.26254	0.1305	37899		
251345849.01	16.059	0.545251	3262.96562	0.0817	139220		
251347050.01	12.290	0.493967	3262.55539	0.0895	17723		
251353301.01	14.556	0.504475	3262.67601	0.0772	87373		
251356484.01	14.484	0.781949	3262.81038	0.1084	186838		
251356953.01	14.568	5.214590	3266.48141	0.1706	555674		
251383916.01	16.220	1.332797	3263.21492	0.1635	645357		
251390801.01	13.319	0.592255	3262.47910	0.0817	312313	twice period	
251393748.01	11.256	8.071810	3266.66297	0.1346	190291		
251393916.01	15.093	0.678473	3262.53788	0.0755	58984		
251394139.01	11.763	26.286249	3277.27748	0.3626	110497		
251404897.01	16.029	0.660085	3262.70281	0.0817	273793		

TABLE 4 — *Continued*

Candidate	Kp	P [d]	T_0 [BJD$_{TDB}$ - 2454833]	T_{14} [d]	$(R_P/R_*)^2$ [ppm]	Comment	Ephemeris matching
251411166.01	14.179	3.374330	3262.71953	0.2550	23276		
251809286.01	16.200	9.485826	3264.49974	0.6392	52542		211738534.01, 211764271.01, 211812160.01
251809628.01	20.140	7.220585	3266.50127	0.2244	38587		211644647.01, 211849962.01, 211852187.01, 211915147.01

TABLE 5
Systems showing periodic variability

Candidate	Kp	P [d]	Comment	Ephemeris matching
211404813.01	16.261	0.560055		211637025.01
211405917.01	16.664	0.537360		
211417284.01	14.388	0.912345		
211419593.01	14.084	0.544223		
211422471.01	9.95	1.694853		
211432103.01	10.249	0.933482	likely even-odd	
211432905.01	17.747	0.565384		
211433054.01	13.798	0.619830		
211434930.01	14.249	0.619451		
211440296.01	15.179	0.494049	thrice period	
211441441.01	16.838	0.591286		
211442676.01	11.446	0.608446		
211443853.01	14.141	0.561341		
211446249.01	14.273	0.615748	four times period	
211446443.01	16.105	0.592558		211733267.01
211448564.01	14.193	0.601654		
211460030.01	14.430	0.645333		
211460061.01	19.164	0.625954		
211461914.01	14.825	0.654160		
211463443.01	12.520	0.616079		211727340.01
211466875.01	11.368	0.652342		
211467499.01	12.702	0.656892		
211469982.01	16.85	0.610206		
211476633.01	14.316	0.593171		
211478023.01	9.328	0.624181	four times period	
211484212.01	16.047	0.560321		
211489039.01	11.760	0.632470		
211490515.01	14.366	1.028101		
211493788.01	15.443	0.505653		
211497766.01	15.273	0.599943		
211500156.01	14.979	0.512656		
211505322.01	14.512	0.636194		
211505333.01	14.727	0.573820		
211513796.01	14.574	0.497528		211830293.01
211514420.01	14.713	0.625234	thrice period	
211515715.01	13.759	0.656366	four times period	
211523002.01	15.759	0.534137		
211532642.01	17.637	0.696100	thrice period.	
211536560.01	16.958	0.549796		
211538914.01	10.110	0.493530		
211548601.01	14.234	0.612276		
211557076.01	13.619	0.757190		
211558647.01	13.173	0.643227	twice period	
211604764.01	15.381	0.631078	double period	
211620946.01	13.789	0.510214	thrice period	
211626641.01	16.243	0.530090		
211630761.01	12.248	0.866331		
211635890.01	14.755	0.725634		
211637025.01	15.064	0.730568		
211637624.01	13.350	0.870809		
211638042.01	15.258	0.549654	thrice period	
211638623.01	15.882	0.930924		
211647067.01	15.508	0.588719	four times period	
211648739.01	11.346	0.543899		
211655464.01	14.846	0.536933		
211660114.01	15.758	0.571957		
211661302.01	14.459	0.729855		
211661627.01	14.265	0.567284	four times period	
211663508.01	14.343	0.544418	four times period	
211663804.01	11.477	0.504537	marginal. twice period	
211665162.01	14.071	0.509189		
211675538.01	10.902	0.942686		
211675809.01	16.992	0.576179	four times period	
211690514.01	14.863	0.543476	twice period	
211690710.01	10.740	0.546275		
211712111.01	14.052	0.578952		
211719362.01	10.481	0.603347	thrice period	
211723397.01	16.886	0.495563		211538914.01, 211723536.01
211723536.01	13.946	0.495561		211536560.01, 211723397.01
211727340.01	16.741	1.201041		
211731135.01	15.656	0.622298		
211740165.01	12.557	0.506108		
211761392.01	15.241	0.651541	period multiple	
211763285.01	13.092	0.504204		
211767109.01	14.050	0.602632		
211796365.01	16.387	0.559817		

TABLE 5 — *Continued*

Candidate	Kp	P [d]	Comment	Ephemeris matching
211812650.01	14.449	0.743778		
211814391.01	15.578	0.514631		
211817361.01	13.595	0.595522		
211821331.01	14.997	0.667574	twice period	
211821355.01	19.48	0.522619		
211836630.01	16.206	0.646600		
211845034.01	16.466	1.332803		
211849962.01	14.307	0.546683		
211856772.01	16.732	0.509990	twice period	
211859760.01	16.567	0.500960		
211862434.01	15.915	0.547386		
211863022.01	14.428	0.805189		
211864337.01	16.056	0.496984		
211869527.01	15.525	1.026173		
211871191.01	16.659	0.558281		
211876205.01	17.528	0.601344		
211880558.01	18.228	0.616146		211404813.01, 211918516.01
211881456.01	17.431	0.588505		
211894518.01	12.214	1.288034		
211902331.01	9.332	1.034110		251350556.02
211907820.01	16.895	1.646612		
211909322.01	15.311	0.838731	twice period	
211911525.01	12.114	0.597831		
211917859.01	17.481	0.574261		
211918335.01	10.042	0.574317		
211918516.01	14.408	0.724075		
211918830.01	12.798	0.692784		
211926098.01	13.349	0.509329		
211926877.01	18.414	0.571362		
211927125.01	11.200	0.680888		
211931604.01	11.827	0.828348	twice period	
211938003.01	15.133	0.630256		
211945144.01	13.940	0.656990	twice period	
211945831.01	14.875	0.516025		
211946241.01	14.332	1.189492		
211947405.01	13.973	0.604689		
211950298.01	16.326	0.510436		
211951418.01	15.433	0.564096		
211957146.01	12.603	0.532536		
211957745.01	16.262	0.507392		
211966619.01	15.166	0.800628		
211996682.01	12.593	1.364680		
212001688.01	14.116	0.796680		
212005402.01	15.052	0.679429		
212008305.01	13.037	0.615002		
212011476.01	12.743	0.715915		
212013694.01	15.313	0.552221		
212018921.01	14.748	0.519797		211911525.01
212018980.01	17.863	0.519707		211902331.01
212019712.01	14.115	0.952995		
212021237.01	18.791	0.681632		
212022582.01	15.127	0.834426		
212024898.01	15.509	0.599922		
212027377.01	17.643	1.106476		
212027952.01	11.290	0.949276		
212028041.01	14.321	0.729797	twice period	
212032754.01	15.853	0.558059		
212037558.01	11.882	0.627062		
212041051.01	16.235	0.627561	four times period	
212043122.01	9.899	0.681463		212013694.01
212048412.01	14.391	0.502575		
212050004.01	16.496	0.681455	twice period	
212050890.01	13.589	0.966599		
212054062.01	16.709	0.944882		
212055545.01	15.058	0.613025		
212060713.01	15.626	0.615370		
212066299.01	11.324	2.609746		
212085240.01	15.164	0.565691		
212086317.01	14.301	0.535092		
212086389.01	16.282	0.493336	thrice period	
212089888.01	15.346	0.681236		
212091210.01	14.526	0.683492		
212091834.01	16.122	0.908531		
212095395.01	10.106	0.640683		
212102092.01	14.613	1.227465		
212105446.01	14.448	0.586443		
212106797.01	15.529	0.614616	twice period	

TABLE 5 — *Continued*

Candidate	Kp	P [d]	Comment	Ephemeris matching
212109327.01	12.477	0.492292		251365170.01, 251365173.01
212110857.01	17.75	0.922879		
212114705.01	19.689	0.610284	twice period	212010565.01
212118200.01	15.204	0.508903		211661627.01
212118344.01	10.719	0.752885		
212159519.01	12.779	0.717385	twice period	
212159586.01	14.621	0.563176		
212161144.01	13.822	0.723318		
212161874.01	16.807	0.572131		
212163652.01	13.465	0.551515		
212164476.01	14.499	0.678440	twice period	
212172621.01	11.764	0.911485		
212174388.01	14.638	0.665443	twice period	
212174434.01	13.481	0.552321	thrice period	
212177756.01	15.782	0.491506		
212180386.01	17.422	0.718264	double period	
212183082.01	17.322	0.575069		
212194110.01	12.819	0.520576		212085240.01
212194171.01	12.819	0.520576		212066299.01
212199005.01	14.449	0.688457		
212204655.01	15.164	0.709082	likely half-period	
212212241.01	15.624	0.618142		
212226872.01	16.140	0.516574		
212230240.01	11.887	0.559411		
251277092.01	12.067	0.502406		
251277701.01	16.014	0.701132		
251278670.01	11.026	0.634153		
251279786.01	16.624	0.503283		
251282021.01	16.240	0.527674		
251283448.01	14.032	0.516848		
251283585.01	15.290	0.497466		
251284270.01	13.642	0.688028		
251284826.01	13.557	0.534658		
251290111.01	16.013	0.515451		
251297292.01	14.451	0.521537	thrice period	
251307454.01	16.142	0.551316		211552050.01
251316666.01	14.396	0.567813		
251321168.01	14.203	0.606779		
251321696.01	15.703	0.631561		
251323035.01	14.221	0.596242	thrice period	
251336933.01	12.952	1.166224		
251342381.01	15.777	0.878144		
251347997.01	14.102	0.497745		
251348935.01	12.852	0.562005		
251349510.01	12.286	0.605516		
251350556.01	16.267	0.699118		
251351108.01	14.098	0.732705		
251355465.01	16.019	0.574342		
251356578.01	11.493	0.788145		
251365170.01	13.313	0.902363		212109327.02,212207368.01, 251365173.01
251365173.01	13.563	0.902431	twice period	212109327.02, 212207368.01, 251365170.01
251374534.01	13.993	0.890305		
251384067.01	17.670	0.527066		
251390658.01	15.332	0.716276		
251391268.01	13.759	0.508759	thrice period	212032754.01
251392383.01	16.699	0.567376		
251397356.01	15.266	1.170258		
251397429.01	12.393	0.542076		
251400494.01	12.922	0.715199	twice period	
251401983.01	14.390	0.836151	twice period	
251402361.01	15.000	0.809957		
251403257.01	16.493	0.638882		
251403570.01	14.633	1.036362		
251809170.01	18.410	0.553061	twice period	
251809263.01	18.930	0.650882		